Ceramics International 51 (2025) 13514–13521

Contents lists available at ScienceDirect

Ceramics International

journal homepage: www.elsevier.com/locate/ceramint

Excellent microwave dielectric properties of novel high-entropy ($Ca_{0.2}Li_{0.2}Sm_{0.2}Mg_{0.2}Zn_{0.2}$) TiO_3 ceramic with dual phase structure

Pengfan Lv [a], Yongping Pu [a,b,*], Xuqing Zhang [a], Xiang Lu [a], Chunhui Wu [a], Lei Zhang [a], Bo Wang [a], Yating Ning [a], Jinbo Zhang [a], Yile Yang [a]

[a] School of Materials Science and Engineering, Shaanxi University of Science & Technology, Xi'an, 710021, China
[b] School of Materials Engineering, Xihang University, Xi'an 710077, China

ARTICLE INFO

Handling Editor: Dr P. Vincenzini

Keywords:
High-entropy
Dual phase
Microwave dielectric properties
Perovskite

ABSTRACT

Novel dual phase high-entropy ($Ca_{0.2}Li_{0.2}Sm_{0.2}Mg_{0.2}Zn_{0.2}$)$TiO_3$ (abbreviated as CLSMZ) microwave dielectric ceramics were synthesized through a solid-state reaction. The study focused on examining the crystal structure, phase composition, microscopic morphology, and vibrational properties of the CLSMZ ceramic. The sintering behavior and its impact on microwave dielectric properties were analyzed using a vector network analyzer, and the results indicated that the microwave dielectric parameters exhibited a rare similar trend. Further analysis found that the dielectric polarizability was the main factor influencing the permittivity (ε_r), while the quality factor ($Q \times f$) was connected with the half-height widths and relative density, and the temperature coefficient of resonance frequency (τ_f) was reliant on the phase composition and crystal structure. The construction of the dual phase high-entropy structure, a novel material design concept, led to the observation of favorable microwave dielectric characteristics with $\varepsilon_r \approx 52$, $Q \times f \approx 10736$ GHz, $\tau_f \approx 40$ ppm/∘C in CLSMZ ceramics sintered at 1275 °C.

1. Introduction

In light of the ongoing advancement of communication technology and the concomitant increase in the number of mobile communication users, high-frequency band microwave was favored for its rapid transmission rate and large communication capacity [1–3]. Microwave dielectric ceramics are essential parts of electronic equipment and indispensable for wireless communication systems and devices worldwide. Generally, they are expected to have a high quality factor [4], which helps enhance frequency selection characteristics and restrain signal attenuation. Furthermore, the devices require the temperature coefficient (τ_f) for resonant frequency that is almost zero, which serves to minimize the fluctuation of the resonant frequency in response to changes in ambient temperature, endowing the device with excellent temperature stability [5]. For another significant parameter, the dielectric constant, on the one hand, given that the time delay of the dielectric resonator is directly correlated with the square root of the permittivity, low ε_r microwave dielectric ceramics are beneficial for reducing the signal propagation delay time [6]. On the other hand, based on the microwave transmission theory, permittivity and resonator size are inversely related, and high ε_r microwave dielectric ceramics is in favour of the miniaturization and integration of the device [7]. Because of these benefits, intermediate ε_r microwave dielectric ceramics have gained a lot of attention in the field of microwave communication.

The three major dielectric parameters of most microwave dielectric materials are typically mutually constrained, particularly permittivity and the quality factor, making it challenging to achieve the ideal values simultaneously [8]. To synchronously enhance the dielectric properties, novel material design strategy are constantly being explored. High-entropy [9–11] has emerged in recent years as a potential novel material design strategy, referring to the formation of solid solutions with five different ion in equiatomic ratios and providing fine regulation through the atomic-scale structure, opening up a new domain for the design of ceramics with excellent properties. Numerous of fields have reported the use of high-entropy strategy, such as ferroelectric [12] and piezoelectric [13], and the outcomes demonstrate that the performance is well optimized. However, the application of high entropy strategy is still lacking in the research field of microwave dielectric ceramics. Xie et al. [14] discovered that the creation of ($Mg_{0.2}Zn_{0.2}Li_{0.4}Ni_{0.2}Co_{0.2}$)$Al_2O_4$ ceramic with spinel type and outstanding performance ($\tau_f \approx -64$

* Corresponding author.
E-mail address: pypelectroceramic@sust.edu.cn (Y. Pu).

https://doi.org/10.1016/j.ceramint.2025.01.194
Received 14 November 2024; Received in revised form 30 December 2024; Accepted 10 January 2025
Available online 10 January 2025

ppm/°C, $\varepsilon_r \approx 7.4$, Q × f ≈ 58,200 GHz) is facilitated by the low average atomic size difference and high configuration entropy; Chen et al. · [15] obtained $(La_{0.2}Nd_{0.2}Sm_{0.2}Ho_{0.2}Y_{0.2})(Nb_{0.8}V_{0.2})O_4$ with $\tau_f = -7.96$ ppm/°C, $\varepsilon_r = 18.14$ and high $Q \times f = 65{,}200$ GHz through a synergistic combination of a high-entropy strategy and substitution of V for Nb; Han et al. [16] found that the trend of microwave dielectric performance of $(Hf_{0.25}Sn_{0.25}Zr_{0.25}Ti_{0.25})O_2$ high-entropy ceramic is closely related to the uniformity of the microstructure. Although these excellent design results provide a solid foundation for the introduction of the high entropy concept in microwave dielectric ceramics. However, it is evident that the current research on high-entropy microwave dielectric ceramics is mainly focused on the design of equivalent elements, single-phase structure and low permittivity, which the medium/high dielectric constant and dual phase high entropy microwave dielectrics remains to be studied. Additionally, the dual phase ceramics can incorporate the advantages of two different crystalline phase ceramics and have extensive research [17–20]. More importantly, in the field of dual phase combined with high entropy [21], Qin et al. [22] et al. prepared ultrahigh-temperature ceramics by dual-phase high-entropy design, expanding existing material systems, Yan et al. [21] prepared dual-phase high-entropy oxide ceramics $(FeCoNiZn)_xV_2O_y$ to enhance electromagnetic wave absorption capabilities, which suggest that the dual-phase high-entropy strategy has significant reference significance.

$CaTiO_3$ with perovskite structure has high permittivity and quality factor, however, on account of its large temperature coefficient, it is not conducive to practical commercial application [23]. Fortunately, a large of studies have found that it has good structural tunability, which is conducive to the substitution of A/B-site cations, this provides the groundwork for the creation of high-entropy ceramics and provides new way to improve the temperature coefficient [24]. The same as the perovskite structure of $Li_{0.5}Sm_{0.5}TiO_3$ have a negative large temperature coefficient, which is often used as a temperature compensator for $CaTiO_3$ to make the temperature coefficient nearly zero [25]. While the combination of Mg^{2+} [26] and Zn^{2+} [27] with Ti^{4+} easily forms a perovskite-like structure with not only negative temperature coefficient, but also ultrahigh quality factor. It can be predicted that the design of Li^{1+}, Sm^{3+}, $Mg^{2+}$and Zn^{2+} elements can make $CaTiO_3$ microwave dielectric ceramics have better property. Hence, guided by the simultaneous improvement of performance, this experiment has designed and prepared middle ε_r dual phase high-entropy CLSMZ ceramics to study their microwave dielectric performance, getting rid of the same valence ions and single-phase high-entropy design ideas.

2. Experimental procedure

Dual phase high-entropy microwave dielectric ceramic $(Ca_{0.2}Li_{0.2}Sm_{0.2}Mg_{0.2}Zn_{0.2})TiO_3$ (abbreviated as CLSMZ) were prepared using the traditional solid-state technique. Raw materials included chemical reagents such as ZnO (99 %), MgO (98.5 %), $CaCO_3$ (99 %), Li_2CO_3 (98 %), Sm_2O_3 (99.99 %) and TiO_2 (98 %). After weighing the oxide powders in a stoichiometric ratio, they were combined with distilled water in a ball milling for 12 h at 400 rpm (grinding media: zirconia balls). The mixture of dried powder was subjected to calcination at 1050 °C for 3 h. The calcined powders were then put through 10 h of ball milling again. The dry powders were compressed into a 14 mm diameter cylindrical billet at a cool isostatic pressure of 200 MPa. Lastly, a sintering process was applied to the compacted pillars for 4.5 h at a temperature between 1225 and 1325 °C.

The X-ray diffractometer (XRD; Rigaku Co) was employed to examine the phase composition and crystal structure of CLSMZ ceramics between the 2θ range from 20° to 80°. Additionally, Raman spectroscopy (Renishaw, UK) was utilized to study ceramic Raman spectra. After the samples were polished, the microstructures, grain sizes, and elemental distributions of the thermally etched surface were studied using an energy dispersive spectrometer-equipped scanning electron microscopy (SEM; S4800, RIGAKU), and the Archimedes technique was used to calculate the bulk density(ρ_{bulk}) of the CLSMZ ceramics. The relative density(ρ_r) was calculated as the followed [28]:

$$\rho_r = \frac{\rho_{bulk}}{\rho_{theo}} \times 100\% \tag{1}$$

where P_{theo} is the theoretical density,it was determined by X-ray diffraction (XRD) data and related analysis software. Frequency and temperature dependence of dielectric performance were acquired through the impedance analyzer (Agilent E4980A). The vector network analyzer (ZNB20, Rohde & Schwarz) was used assess dual phase high-entropy CLSMZ ceramics' microwave dielectric characteristics. The method of resonant cavity was used to determine ε_r and $Q \times f$ of CLSMZ ceramic, while the Hakki-Coleman approach was utilized to determine the τ_f for a 25–85 °C temperature range of,the formula for this method is as follows:

$$\tau_f = \frac{f_1 - f_0}{f_0(T_1 - T_0)} \tag{2}$$

where the resonance frequencies were f_0 and f_1 at 25 °C (T_0) and 85 °C (T_1).

3. Results and discussion

Generally, according to the value of ΔS_{config}, materials can be defined as high entropy (1.5 R ≤ ΔS_{config}), medium entropy (1R ≤ ΔS_{config}≤ 1.5 R) and low entropy (ΔS_{config} ≤ 1R) materials, the ΔS_{config} can be calculated by following formula [29]:

$$\Delta S\_(\text{config}) = -\mathrm{R}\left[\left(\sum_{a=1}^{n} x_a \ln x_a\right)_{\mathrm{A-site}} + \left(\sum_{b=1}^{n} x_b \ln x_b\right)_{\mathrm{B-site}} + 3\left(\sum_{c=1}^{n} x_C \ln x_c\right)_{\mathrm{O-site}}\right] \tag{3}$$

where R is the ideal gas constant, x_a, x_b and x_o are the mole fractions of A, B and O site, respectively. The calculated entropy of CLSMZ microwave dielectric ceramics is expeed 1.5R, which indicates that it belongs to the range of high entropy ceramics and it is conducive to improving the comprehensive properties of ceramics. Fig. 1a illustrates the XRD patterns of dual phase high-entropy CLSMZ microwave dielectric ceramics, which were synthesized at sintering temperatures ranging from 1225 to 1325 °C. The diffraction peaks agreed well with the standard PDF cards (PDF#86–1393) and (PDF#87–1781), indicating a stable complex structure composed of $CaTiO_3$ and $Zn_2Ti_3O_8$, and the high entropy strategy results in excellent temperature stability. In order to further investigate the phase composition, we Rietveld refinement on the material, and the results are shown in Fig. 1b, and the reliability of the results is ensured by $R_{WP} = 4.78$ %. $CaTiO_3$ exhibits a perovskite structure [30], while $Zn_2Ti_3O_8$ has a spinel structure, leading to variations in the degree of deformation of their octahedra. The significant difference in ionic radii between Ca^{2+} (1.34 Å) and Zn^{2+} (0.74 Å) occupying the a-site results in limited solid solubility [18], the differences in ionic size and crystal structure account for the coexistence of the two phases.

Fig. 2 presents the SEM images of the thermally etched surfaces of dual phase high-entropy CLSMZ ceramic after polishing. At a sintering temperature of 1225 °C, the samples exhibit fine grains, as the sintering temperature increases, the grains undergo gradual growth, resulting in a comparatively dense microstructure. However, at 1325 °C, over-sintering leads to the formation of air holes, indicating that the micromorphology of ceramic samples is significantly influenced by the sintering temperature [31,32]. Additionally, SEM images reveal two distinct sizes and colors of grains, in order to investigate the cause of their formation and further confirm the phase composition of high-entropy CLSMZ ceramics, energy spectrum analysis was conducted as shown in Fig. 2f. The results reveals that the light-coloured regions

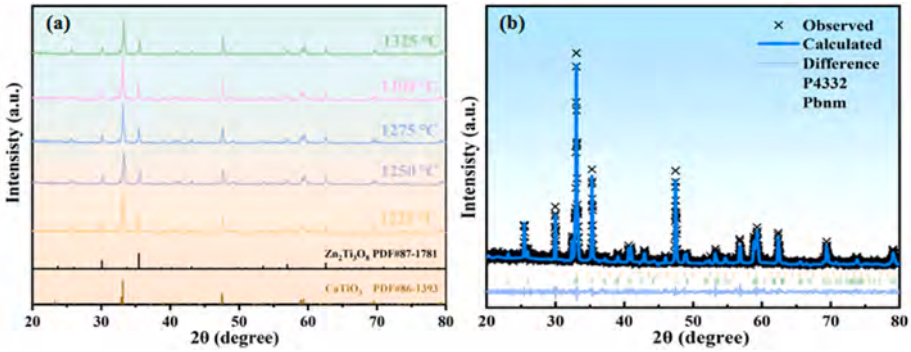

Fig. 1. (a)XRD patterns of CLSMZ ceramics between the 2θ range from 20∘to 80° (b)Rietveld refinement result of CLSMZ ceramic sintered at 1275 °C.

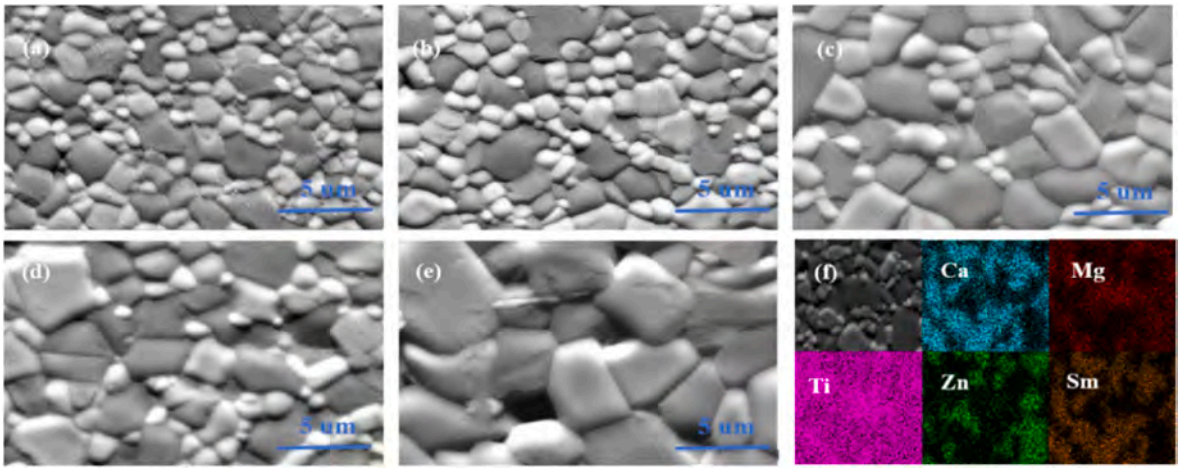

Fig. 2. SEM images of CLSMZ ceramics at different sintere temperatures(a)1225 °C, (b)1250 °C, (c)1275 °C, (d)1300 °C, (e)1325 °C and (f) EDS mapping of CLSMZ ceramics sintered at 1275 °C.

are enriched with Ca^{2+} and Sm^{3+}, it may be caused by $CaTiO_3$ and $Li_{0.5}Sm_{0.5}TiO_3$ of perovskite structure, and whereas the darker regions correspond mainly to Zn^{2+} and Mg^{2+}, which confirms the dual phase's structure and is in line with the X-ray diffraction data.

Combined with scanning electron microscope images, the mean grain size and dispersion of CLSMZ ceramics at various temperatures were evaluated and analyzed with nano-measure software, as depicted in Fig. 3. The average grain size of CLSMZ microwave dielectric ceramics

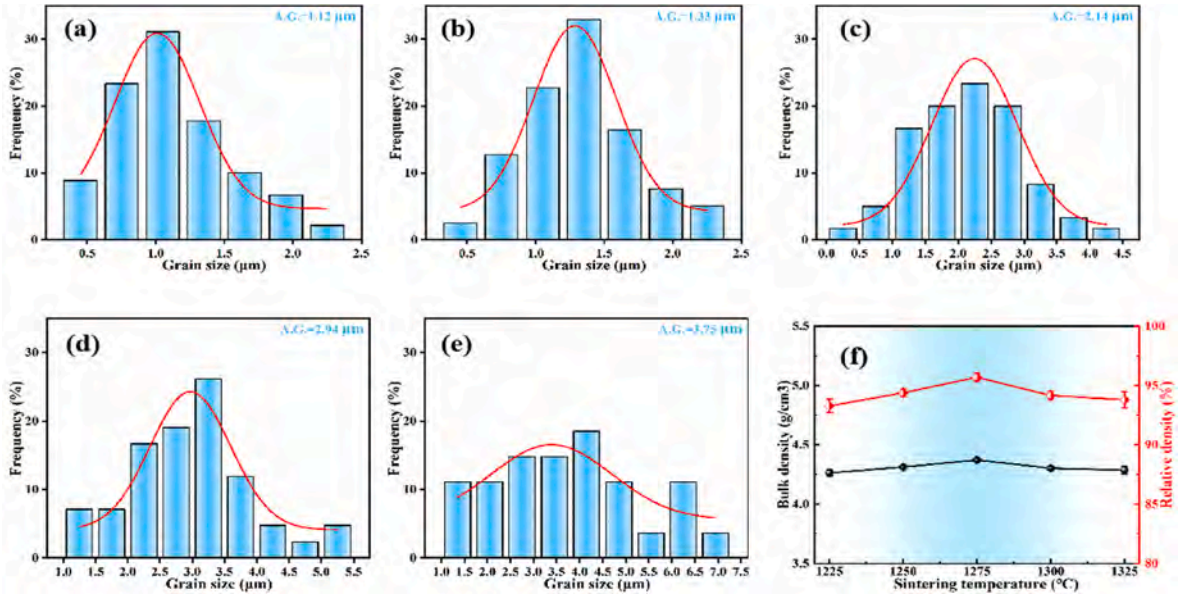

Fig. 3. Grain size distribution and average grain size of CLSMZ ceramics sintered at: (a) 1225 °C, (b) 1250 °C, (c) 1275 °C, (d) 1300 °C, (e) 1325 °C and (f) the density of CLSMZ ceramics.

increased from 1.12 μm to 3.75 μm as sintering temperature rose, indicating progressive grain growth [19,33]. The grain size distribution from 1225 to 1300 °C followed a normal distribution ($r^2 > 0.85$) with a small standard deviation, suggesting uniform grain growth [34]. However, at a sintering temperature of 1325 °C, anomalous grain growth occurs, deviating from the expected normal distribution. This is evidenced by the emergence of substantial grains, reaching a maximum size of 6.95 μm, consistent with SEM observations. In addition, the grain size of CLSMZ is significantly reduced compared to the grain size of $CaTiO_3$, which can be caused by the hysteretic diffusion effect of high entropy ceramics. Chen et al. [35] reported that changes in microstructure such as grain, distribution and porosity affect the overall performance of the material, especially its density. As shown in Fig. 3f, before reaching the optimal sintering temperature, relative density increases with grain growth. However, as the temperature continues to rise, the generation of pores leads to a decrease in relative density.

Similar trends are seen in the Raman spectra of dual phase high-entropy CLSMZ ceramics, as shown in Fig. 4a, suggesting that the samples showcase outstanding phase structure stability at diverse temperatures. Eight Raman modes are revealed by the fitting results of the Raman spectra, which are displayed in Fig. 4b. It is likely that some peaks were not detected due to the low resolution of the instrument, or that some specific Raman modes have relatively low intensity [36]. The majority of research [18,37–39] in the ABO_3 perovskite microwave dielectric ceramics indicates that the A-site atoms vibrations are responsible for the peaks seen below 180 cm^{-1}. The internal vibration and rotation of the TiO_6 octahedra are responsible for the peaks observed within the ranges of 200–400 cm^{-1} and 400–600 cm^{-1}, where the Raman peak at 330 cm^{-1} pertains to Rotations of the oxygen octahedral, the peak at 476 cm^{-1} relates to internal vibration of oxygen octahedral, the peak at 533 cm^{-1} relates to Ti-O stretching vibration, the Raman peak at 650 cm^{-1} is associated with lattice defects. The pattern of the peak at 784 cm^{-1} is regarded as the A_{1g} mode and corresponds to breathing vibrations of the TiO_6 octahedron [40]. In short, the outcomes of Raman analyses manifested the phase structure stability of dual phase high-entropy composite CLSMZ ceramics and offered valuable perceptions into the structural properties and vibrational modes of the material [1,41].

Fig. 5a illustrates the temperature dependent relative permittivity and loss of dual phase high-entropy CLSMZ ceramics sintered at 1275 °C across different frequencies. With the temperature increases, both permittivity and loss exhibit an upward trend. It is possible that with the temperature rises, the thermal motion of molecules may accelerate and oxygen vacancies is generated by thermal activation [42]. Fig. 5c depicts the change in permittivity and loss with frequency, it decreases significantly from 100 Hz to 1 MHz, this change can be linked to variations in four fundamental mechanisms influence polarization, each characterized by its own natural frequency and intrinsic response time. At low frequencies, all types of polarization are capable of responding to the fluctuations of the external electric field, thereby contributing to an increased ε_r value. As the electric field frequency steadily increases, however, the polarization mechanisms require more time and eventually fail to keep pace with these changes, causing the dielectric constant to decrease [43]. In addition, we found that both in the dielectric temperature and in the dielectric spectrum, samples sintered at 1275 °C exhibited the highest permittivity alongside low dielectric loss, this could also be the cause of the CLSMZ ceramic sintered at 1275 °C have best microwave dielectric characteristics.

Fig. 6 displays the relative permittivity (ε_r) of dual phase high-entropy CLSMZ ceramics sintered at different temperatures. Generally, the relative permittivity is affected by internal and external factors, internal factors such as ionic polarization rate [44], ordering degree [45], chemical bonds and lattice energies [46], external factors such as density, the external dielectric contributions from the defects [47] and the second phase [48]. It can be found that the ε_r increases monotonically from 48 at 1225 °C to a maximum value of 52 at 1275 °C, then decrease to 49 at 1325 °C. This trend is consistent with the observed relative density, suggesting that density of CLSMZ ceramics affects their ε_r value [8]. Furthermore, it has been reported that the presence of porosity (P) significantly impacts the final ε_r value. To investigate the factors affecting ε_r more accurately, using the Bosman-Having approach, the ε_r value was corrected [49].

$$\varepsilon_{corr.} = \varepsilon_{mea.}\ (1 + 1.5P) \tag{4}$$

$$P = (1 - \rho_{relative}) \tag{5}$$

where P is the porosity fraction. The dielectric constant corrected ($\varepsilon_{corr.}$) for P and porosity is shown in Fig. 6. It can be observed that throughout the range of sintering temperatures, ε_r and $\varepsilon_{corr.}$ exhibit a similar trend, while showing an inverse relationship with P. The sintered samples demonstrate a stable ε_r value of approximately 49, except at 1275 °C, indicating that porosity is a significant factor in determining the ε_r value.

On the other hand, according to the Clausius-Mosotti (C-M) equation and the mixing rule [47], the dielectric constant of a material is closely related to its ionic polarizability and phase composition:

$$\varepsilon_{theo} = \frac{3Vm + 8\pi\alpha_{theo}}{3Vm - 4\pi\alpha_{theo}} \tag{6}$$

$$\ln \varepsilon_{theo} = V1 \bullet \ln\bullet_{theo1} + V2\ln\bullet_{theo2} \tag{7}$$

where V_m and α_D represent the molar volume and dielectric polarizability, ε_1 and ε_2 denote the corresponding theoretical permittivities; V_1 and V_2 represent the volume fractions of the phases, respectively. Shannon put forth that polarizabilities of the constituent ions can be used to estimate the molecular polarizability (α) of a given compound. For $(Ca_{0.2}Li_{0.2}Sm_{0.2}Mg_{0.2}Zn_{0.2})TiO_{3theo}$,

$$\alpha((Ca_{0.2}Li_{0.2}Sm_{0.2}Mg_{0.2}Zn_{0.2})\ TiO_3 = 0.2 \times (\alpha_{Ca}^{2+} + \alpha_{Li}^{1+} + \alpha_{Sm}^{3+} + \alpha_{Mg}^{2+} + \alpha_{Zn}^{2+}) + \alpha_{Ti}^{4+} + 3 \times \alpha_{O}^{2-}$$

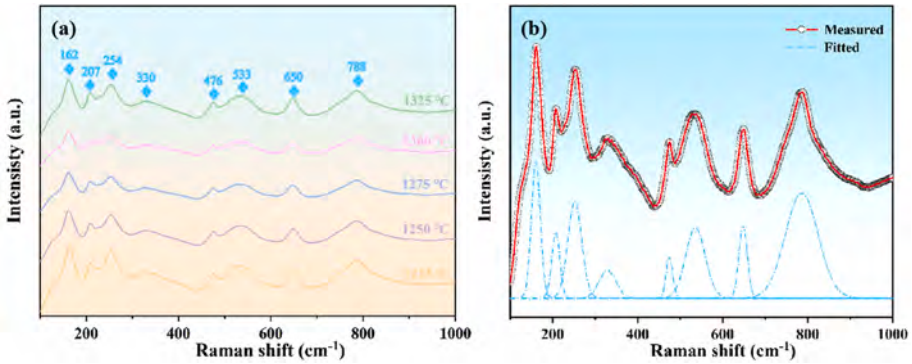

Fig. 4. (a) Raman spectra of CLSMZ ceramics sintered at different temperatures; (b) Fitted curve for CLSMZ ceramics sintered at 1275 °C.

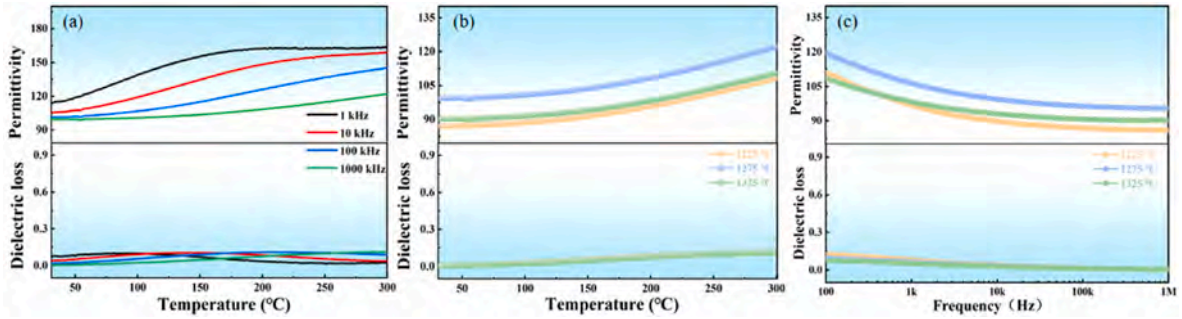

Fig. 5. (a) Temperature dependence of the dielectric constant and dielectric loss of CLSMZ ceramic sintered at 1275 °C across different frequencies (b-c)Temperature and Frequency dependence of CLSMZ ceramics.

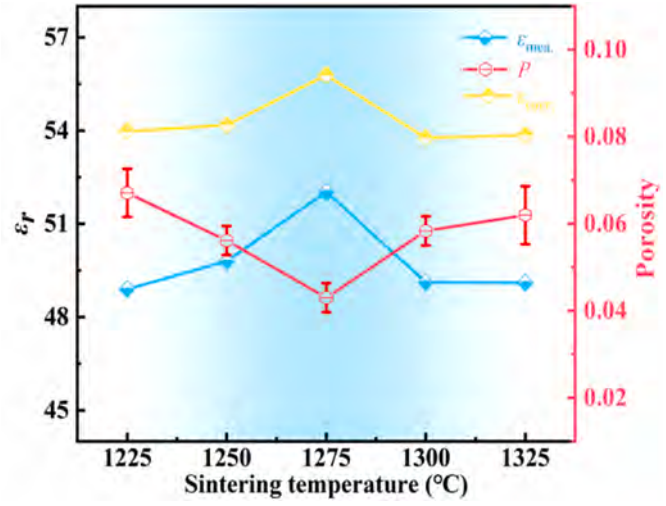

Fig. 6. ε_r and P of CLSMZ ceramics as a function of sintering temperature.

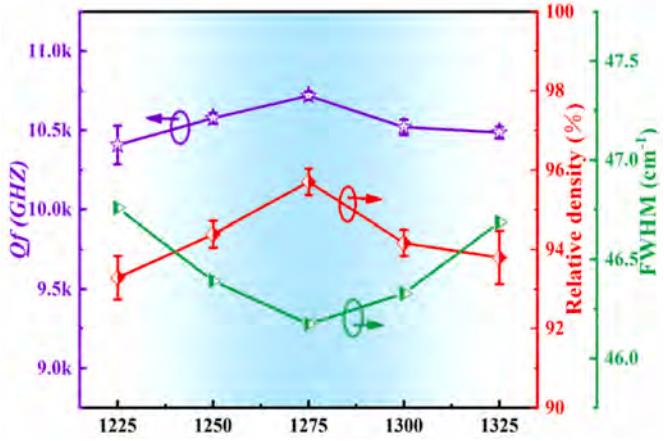

Fig. 7. Variation trends in $Q \times f$, FWHM and Relative density of CLSMZ ceramics.

and the α of Ca^{2+}, Mg^{2+}, Li^{1+}, Sm^{3+}, Zn^{2+}, Ti^{4+}, and O^{2-} are 3.17, 1.2, 4.74, 1.33, 2.09, 2.94 and 2.01 Å^3, respectively. The α_D value is 11.476 Å^3, and the ion polarization rate significantly influences the dielectric constant in the microwave frequency range. This is due to in this frequency dipole polarization and space charge polarization lag behind the frequency response and ion displacement alters the charge distribution within the material, leading to an enhanced local electric field, thus in general the larger ion polarization lead the larger dielectric constant. Suitable dielectric polarizability is also one of the important reasons for its medium permittivity, this facilitates it to meet its miniaturization and faster transmission at the same time.

It is common knowledge that the $Q \times f$ is predominantly influenced by both intrinsic and non-intrinsic losses [50,51]. Intrinsic losses are primarily attributable to internal lattice vibrations, stacking fractions and phase compositions. In contrast, grain size, densification, lattice flaws, and impurities are the principal causes of non-intrinsic losses. The change patterns of the $Q \times f$ value, relative density (ρ_r) and half-height width at the Raman frequency shift of CLSMZ samples with sintering temperature are given in Fig. 7. When the sintering temperature progressively increases, the $Q \times f$ exhibits an initial increase, followed by a decline, reaching a maximum value (10736 GHz) at 1275 °C. This trend is consistent with the majority of reported observations, whereby the $Q \times f$ value is inversely proportional to the change in half-height width and proportional to the relative density variation. The half-height width of the Raman characteristic peak is a significant parameter in evaluating the intrinsic loss of the ceramic [52]. It is associated with the damping factor and is influenced by the crystallinity and defects of the ceramics. Smaller half-height widths result in enhanced lattice vibrations, which enhance the crystallinity of the sample, lessen the dielectric loss while improve the quality factor.

In addition, the correlation between the quality factor with the grain size and distribution has also been documented. Usually, a reduction in grain size is associated with an increase in grain boundary density, which can result in enhanced microwave refraction or reflection at grain boundaries as well as a loss of microwaves during transmission, this is disadvantageous for the $Q \times f$. Consequently, prior to the optimal temperature, the grain boundaries decrease and the quality factor increases as the grain grow [53]. As the temperature of sintering is raised further, although the grain continue to grow,the appearance of pores and the weakening of the lattice vibrations due to overfiring lead to a reduction in relative density and an increase in FWHM, which has a vital detrimental impact on the $Q \times f$ [31]. It is noteworthy that the dielectric constant and quality factor exhibits a similar trend, which is rare in microwave dielectric ceramic materials, where the key performance parameters are mutually restricted, and this further illustrates the significant influence of the dual phase high entropy structure and relative density on the dielectric properties.

The CLSMZ ceramic's τ_f values demonstrate a temperature-dependent variation, as shown in Fig. 8. It can be observed that how the τ_f varies with the sintering temperature exhibits less sensitive compared to other ceramics, with no apparent change. This observation suggests that the dual phase high-entropy CLSMZ ceramic exhibits remarkable temperature stability [54]. It is commonly recognized that the crystal structure of perovskite-type microwave dielectric ceramics, in particular the distortion of oxygen octahedrons, has a considerable impact on the τ_f [55]. In the case of CLSMZ high-entropy ceramics, the random occupation of the A-site by Ca^{2+}, Li^{1+}, Sm^{3+}, Mg^{2+} and Zn^{2+} cations, which causing lattice distortion and reducing the extent of octahedral deformation of oxygen, thereby enhancing the material's

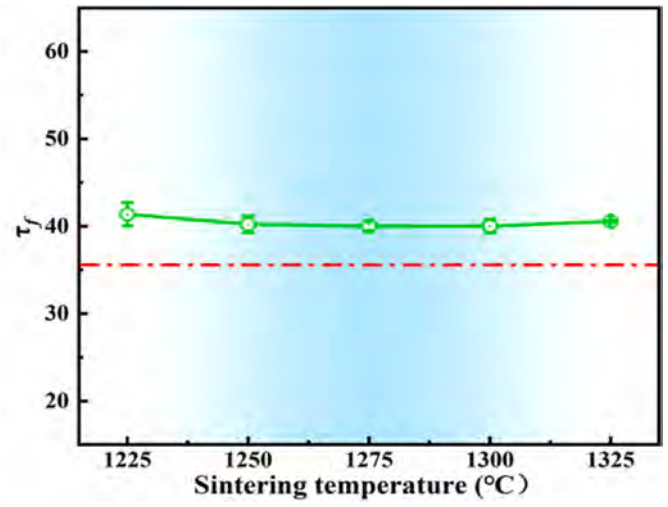

Fig. 8. τ_f of CLSMZ ceramics as a function of sintering temperature.

stability. This may also be a contributing factor to the excellent microwave dielectric properties observed [56]. Furthermore, based on the aforementioned formula:

$$\tau_f = v_1 f_1 + v_2 f_2 \tag{8}$$

we have calculated that the theoretical τ_f value of CLSMZ ceramics and can be found that the properties of our prepared ceramics are close to the theory, this proves the success of our multiphase high-entropy design [36].

Impedance spectroscopy represents a significant tool for elucidating mechanism of dielectric response and has been increasingly employed in the analysis of microwave dielectric ceramics. Fig. 9a illustrates the relationship between the impedance's imaginary (Z″) and real (Z′) components at varying test temperatures with CLSMZ ceramics, wherein all ceramics exhibit a single Debye semicircle. It is evident that the radius of this semicircle decreases in proportion to an increase in test temperature. This indicates reduction in the resistance of the ceramics and resistance exhibits a negative temperature coefficient, suggesting that as test temperatures rise, excess charge carriers are produced within the ceramic to engage in conductive processes, thereby influencing its dielectric performance [57]. In addition, where the illustration in Fig. 9b, the radius of the semicircle increases at first and then decreases as the sintering temperature rises. The sintered sample at 1275 °C exhibits the largest semicircle, indicating that it possesses the most optimal insulating properties. The impedance across all ceramics was observed to vary with temperature, demonstrating significant thermal stability and suggesting the presence of thermally activated processes. Application of the Arrhenius equation can determine the activation energy of CLSMZ ceramics.:

$$\sigma = \sigma_0 \, exp\left(-\frac{Ea}{k_B T}\right) \tag{9}$$

whereσ_0 is the pre exponential term, and the absolute temperature is represented by T. The variation curve for CLSMZ ceramics between 1000/T and ln(σ) is displayed in Fig. 9c. Ea has a tendency to rise and then down, This surge in Ea correlates with a reduction in oxygen vacancies [58], this leads to a reduction in the ceramic's non-intrinsic loss. Therefore, the CLSMZ sample sintered at 1275 °C has the smallest loss, resulting in the largest $Q \times f$.

Fig. 10 compares the ε_r, $Q \times f$ and τ_f of this study with reference those of other novel microwave dielectric ceramics [59–66]. It is noteworthy that the CLSMZ ceramics under investigation exhibit not only elevated of the ε_r and the $Q \times f$, but also a relatively low τ_f, which is indicative of superior performance compared to other recently discovered microwave dielectric ceramics. In general, microwave dielectric ceramics with medium to high permittivity tend to exhibit poor loss and stability due to their large dielectric constant. This results in a low quality factor as well as coefficient temperature stability. Furthermore, the dielectric performance of microwave materials is typically mutually exclusive, which presents a significant challenge in achieving optimal performance simultaneously. Nevertheless, the successful attainment of these two properties in our study offers valuable insights that can direction of future research into microwave dielectric ceramics. In addition, high entropy strategies generally enhance the mechanical properties of ceramics. Xie et al. [67] and Liu et al. [29] have significantly suggested the compressive strength of high-entropy alloys and ceramics through the regulation of configurational entropy; Feng et al. [21] significantly increased the Vickers hardness of (Cr, Hf, Nb, Ta, Ti, Zr)B_2-(Cr, Hf, Nb, Ta, Ti, Zr)C ceramics through the design of multi-phase high-entropy. The mechanical properties of the CLSMZ ceramic have been tested and

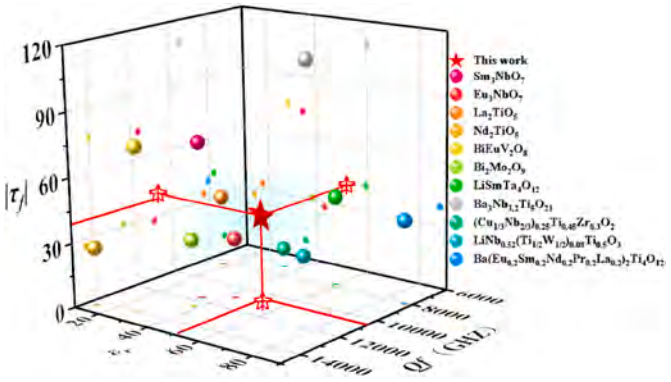

Fig. 10. Comparison between the performance observed in this study and that reported for novel medium dielectric constant microwave dielectric ceramics in recent years.

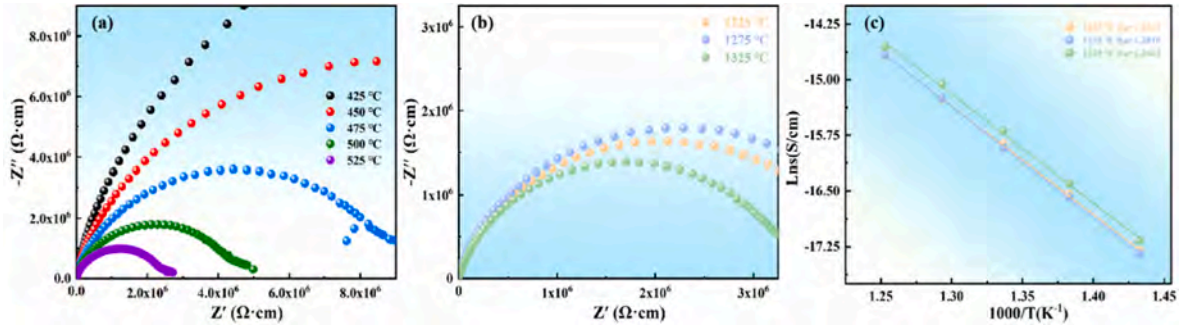

Fig. 9. Complex impendence spectra of CLSMZ ceramics (a)sintered at 1275 °C from 450 to 550 °C(b)sintered at 1225 °C, 1275 °C and 1325 °C (c) Fitted pattern of ln(σ) versus 1000/T for CLSMZ ceramics.

the results show that it has a high compressive strength of approximately 517 Mpa, which enhances its applicability in harsh environments. Therefore, the enhancement of CLSMZ's microwave dielectric and mechanical properties may result from the synergistic effects of high entropy strategies combined with complex phase structures.

4. Concusion

In summary, A novel design concept based on dual phase and high-entropy is proposed, leading to the successful preparation of innovative CLSMZ microwave dielectric ceramics with outstanding performance through a traditional solid-state reaction technique. Compared with $CaTiO_3$ microwave dielectric ceramics with normal performance ($\varepsilon_r \approx 170$, $Q \times f \approx 3500$ GHz, $\tau_f \approx +800$ ppm/∘C), the optimal performance ($\varepsilon_r \approx 52$, $Q \times f \approx 10736$, $\tau_f \approx 40$ ppm/°C) were obtained when sintered at 1275 °C due to the incorporation of five cations, Ca^{2+}, Li^{1+}, Sm^{3+}, Mg^{2+} and Zn^{2+} occupied the A sites via dual phase high-entropy composition design, which affected the oxygen octahedron distortiond. Furthermore, the ε_r, $Q \times f$, and τ_f are primarily governed by factors such as dielectric polarizability, relative density, half-height,phase composition and crystal structure in dual phase high-entropy CLSMZ ceramics. The outstanding microwave dielectric performance render complex microwave high-entropy CLSMZ ceramics exemplary candidates for applications in microwave communication technologies. Additionally, this innovative design concept provides certain reference that may facilitate future advancements in the development of microwave dielectric ceramics.

CRediT authorship contribution statement

Pengfan Lv: Writing – original draft, Methodology, Investigation, Data curation, Conceptualization. **Yongping Pu:** Writing – review & editing, Methodology, Funding acquisition, Formal analysis, Conceptualization. **Xuqing Zhang:** Investigation, Formal analysis, Conceptualization. **Xiang Lu:** Validation, Software. **Chunhui Wu:** Validation, Software. **Lei Zhang:** Supervision, Resources. **Bo Wang:** Supervision, Resources. **Yating Ning:** Software, Methodology. **Jinbo Zhang:** Software, Methodology. **Yile Yang:** Software.

Declaration of competing interest

The authors declare that they have no known competing financial interests or personal relationships that could have appeared to influence the work reported in this paper.

Acknowledgments

This work was financed by the National Natural Science Foundation of China (No. 52172118).

References

[1] L. Xiao, L.W. Deng, Y.X. Li, Z.J. Qing, Y.C. Xi, J.H. Zhu, S. Peng, A $TiSnNbTaGa_2O_{12}$ high-entropy microwave dielectric ceramic with rutile structure and near-zero τ_f, J. Eur. Ceram. Soc. 44 (2024) 277–283.
[2] J.P. Yuan, B. Liu, C.C. Hu, K.X. Song, Y.H. Huang, Reactive cold sintering of dense barium sulfate ceramics for high-reliability chip packaging in integrated circuits, J. Eur. Ceram. Soc. 44 (2024).
[3] X. Lu, Y.P. Pu, C.H. Wu, Y.X. Hao, P.F. Lv, Y.Q. Yang, L. Zhang, B. Wang, Effect of analogue nucleating agent on the interface polarization and energy-storage performance of $NaNbO_3$-based glass-ceramics, Ceram. Int. 50 (2024) 44503–44510.
[4] Y.M. Lai, X.L. Tang, H.W. Zhang, X.F. Liang, X. Huang, Y.X. Li, H. Su, Correlation between structure and microwave dielectric properties of low-temperature-fired Mg_2SiO_4 ceramics, Mater. Res. Bull. 99 (2018) 496–502.
[5] K. Du, X.Q. Song, Z.Y. Zou, J. Fan, W.Z. Lu, W. Lei, Improved microwave dielectric properties of novel low-permittivity Sn-doped $Ca_2HfSi_4O_{12}$ ceramics, Mater. Res. Bull. 129 (2020).
[6] F.S. Wang, Y.M. Lai, Q. Zhang, X.Z. Yang, B.Y. Li, C.S. Wu, H. Su, Improved microwave dielectric properties of $(Mg_{0.5}Ti_{0.5})^{3+}$ Co-substituted $Mg_2Al_4Si_5O_{18}$ cordierite ceramics, Solid State Sci. 132 (2022).
[7] W.J. Guo, Z.Y. Ma, Y. Luo, Y.G. Chen, Z.X. Yue, L.T. Li, Structure, defects and microwave dielectric properties of Al-doped and Al/Nd Co-doped $Ba_4Nd_{9.33}Ti_{18}O_{54}$ ceramics, J. Adv. Ceram. 11 (2022) 629–640.
[8] H. Tian, X.H. Zhang, W. Du, Z.B. Feng, L.G. Wang, H.T. Wu, W.S. Xia, Structure characteristics and microwave/terahertz dielectric response of low-permittivity $(La_{0.2}Nd_{0.2}Sm_{0.2}Eu_{0.2}Gd_{0.2})_2Zr_3(MoO_4)_9$ high-entropy ceramics, Ceram. Int. 50 (2024) 6403–6411.
[9] J.W. Ye, S.K. Chen, S.J. Lin, J.Y. Gan, T.S. Chin, T.T. Shun, Nanostructured high-entropy alloys with multiple principal elements: novel alloy design concepts and outcomes, Adv. Eng. Mater. 6 (2004) 299–303.
[10] K. Liu, H.W. Zhang, C. Liu, J. Li, L. Shi, X.Y. Wang, D.N. Zhang, Crystal structure and microwave dielectric properties of $(Mg_{0.2}Ni_{0.2}Zn_{0.2}Co_{0.2}Mn_{0.2})_2SiO_4$ - a novel high-entropy ceramic, Ceram. Int. 48 (2022) 23307–23313.
[11] Y.T. Ning, Y.P. Pu, X.Q. Zhang, Z.M. Chen, C.H. Wu, L. Zhang, B. Wang, X. Li, Remarkable energy-storage density together with efficiency of above 92% in high-entropy ferroelectric ceramics, Mater. Today Phys. 43 (2024).
[12] Z.M. Chen, Y.P. Pu, Y.T. Ning, Y.T. Hui, C.H. Wu, L. Zhang, X.Q. Zhang, B. Wang, Prominent energy storage density and efficiency of $Na_{0.5}Bi_{0.5}TiO_3$-based ceramics via multiscale amelioration strategy, J. Am. Ceram. Soc. 107 (2023) 2360–2370.
[13] Y. Liu, J.Y. Yang, S.Q. Deng, Y.Y. Zhang, Y.C. Zhang, S.D. Sun, L. Wang, Flexible polarization configuration in high-entropy piezoelectrics with high performance, Acta Mater. 236 (2022).
[14] M. Xie, X. Li, Y.M. Lai, C. Qi, J. Yin, W.P. Gong, Phase evolution and microware dielectric properties of high-entropy spinel-type $(Mg_{0.2}Co_{0.2}Ni_{0.2}Li_{0.4}Zn_{0.2})Al_2O_4$ ceramics, J. Eur. Ceram. Soc. 44 (2024) 284–292.
[15] D.Q. Chen, X.W. Zhu, S.Y. Xiong, G.B. Zhu, L.J. Liu, J. Khaliq, C.C. Li, Microwave dielectric properties in rare-earth niobates via a high-entropy configuration strategy to induce ferroelastic phase transition, ACS Appl. Mater. Interfaces 15 (2023) 52776–52787.
[16] Y.H. Ding, L. Liu, R.Z. Guo, L. Li, X.M. Chen, $(Hf_{0.25}Zr_{0.25}Sn_{0.25}Ti_{0.25})O_2$ high-entropy ceramics and their microwave dielectric characteristics, J. Am. Ceram. Soc. 105 (2022) 6710–6717.
[17] X. Chen, F. Wang, X. Zhang, S.S. Hu, X.B. Liu, S. Humphry-Baker, Novel refractory high-entropy metal-ceramic composites with superior mechanical properties, Int. J. Refract. Met. Hard Mater. 119 (2024).
[18] C.H. Wu, Y.P. Pu, X. Lu, Y.T. Ning, B. Wang, L. Zhang, Z.M. Chen, Y.Q. Yang, Constructing novel $SrTiO_3$-based composite ceramics with high energy storage performance under moderate electric field, J. Power Sources (2024) 604.
[19] T. Shi, F. Zhang, W.Y. Sun, J.R. Li, Y. Bai, C. Wang, X. Wang, Y.H. Yang, Fabrication, sinterability and microwave dielectric properties of $MgTiO_3$-$(Ca_{0.8}Sr_{0.2})TiO_3$ composite ceramics from nanosized powders, Vacuum (2022) 201.
[20] C.H. Wu, Y.P. Pu, X. Lu, Y.T. Ning, L. Zhang, B. Wang, Z.M. Chen, P.F. Lv, Y. Q. Yang, Z. Wang, Innovative binary $Na_{0.5}Bi_{0.5}TiO_3$-based composite ceramics with excellent comprehensive energy storage performances under low electric fields, Composites, Part B 288 (2024).
[21] Z.K. Yan, D.P. Li, X. Zhang, Q.Q. Men, B.B. Fan, L. Guan, X.Q. Guo, R. Zhang, B. Zhao, Dual-phase high-entropy $(FeCoNiZn)_xV_2O_y$ oxides with promising microwave absorption properties, Ceram. Int. 48 (2022) 36871–36879.
[22] M.D. Qin, J. Gild, C.Z. Hu, H.R. Wang, J. Luo, Dual-phase high-entropy ultra-high temperature ceramics, J. Eur. Ceram. Soc. 40 (2022) 5037–5050.
[23] A. Zhang, H.Q. Fan, D.W. Hou, X. Meng, W.J. Wang, Structure-dielectric property relations in $(Al_{0.5}Nb_{0.5})^{4+}$ co-doped $Ca_{0.8}Sr_{0.2}TiO_3$ ceramics with excellent temperature stability, Ceram. Int. 48 (2022) 34323–34331.
[24] P. Zhang, Z.H. Lou, M.J. Qin, J. Xu, J.T. Zhu, Z.M. Shi, Q. Chen, M.J. Reece, High-entropy$(Ca_{0.2}Sr_{0.2}Ba_{0.2}La_{0.2}Pb_{0.2})TiO_3$ perovskite ceramics with A-site short-range disorder for thermoelectric applications, J. Mater. Sci. Technol. 97 (2022) 182–189.
[25] D.Y. Zhang, H. Hao, Y.S. Luo, Z.H. Yao, M.H. Cao, H.X. Liu, Effect of ZnO doping on the microstructure and microwave dielectric properties of $0.2CaTiO_3$-0.8 $(Li_{0.5}Sm_{0.5})TiO_3$ ceramics, Ceram. Int. 48 (2022).
[26] B.Y. Li, Y.M. Lai, Y.M. Zeng, F. Yang, F.Y. Huang, X.Z. Yang, F.S. Wang, C.S. Wu, X. L. Zhong, H. Su, Structure and microwave dielectric properties of $(Zn_{1/3}Nb_{2/3})^{4+}$ co-substituted $MgTiO_3$ ceramic, Mater. Sci. Eng. 276 (2022).
[27] S.P. Wu, J.H. Luo, S.X. Cao, Microwave dielectric properties of B_2O_3-doped $ZnTiO_3$ ceramics made with sol-gel technique, J. Alloys Compd. 502 (2010) 147–152.
[28] L. Cao, Y.Y. Wang, X.Q. Yu, Z.L. Lu, G. Wang, M.M. Mao, B. Liu, L. Cao, K.X. Song, Significantly enhanced microwave-millimeterwave properties of cordierite ceramics: roundness regulation of Si-Al hexagonal ring, analysis of far-infrared reflectance and terahertz time-domain spectroscopy, J. Eur. Ceram. Soc. 45 (2025).
[29] B. Liu, F.L. Lin, K.X. Song, Y.H. Huang, Resolving the role of configurational entropy in the optimization of mechanical, thermal, and microwave dielectric properties of $SrLa(Al_{0.50-x}Ga_xZn_{0.125}Mg_{0.125}Ti_{0.25})O_4$ ceramics, ACS Appl. Mater. Interfaces 16 (2024) 55747–55750.
[30] X.Q. Zhang, Y.P. Pu, Y.T. Ning, L. Zhang, B. Wang, Z.M. Chen, Ultrahigh energy storage with superfast charge-discharge capability achieved in linear dielectric ceramic, J. Mater. Sci. Technol. 177 (2024) 59–67.
[31] Y.X. Li, W. Liu, X.Y. Pang, A. Oad, D.Y. Liang, Microwave dielectric properties, Raman spectra and sintering behavior of novel low loss $La_7Nb_3W_4O_{30}$ ceramics with rhombohedral structure, Ceram. Int. 50 (2024) 25918–25924.
[32] J.B. Zhang, Y.P. Pu, Y.X. Hao, Y.L. Yang, L. Zhang, B. Wang, Q. Pan, Realizing excellent energy-storage performance under low electric fields in lead-free $BiFeO_3$-$BaTiO_3$-based ceramics with ultrahigh polarization difference, J. Energy Storage 105 (2025).

[33] X. Peng, Y.P. Pu, X.Y. Du, Y.X. Hao, Optical transmittance and energy storage properties of potassium sodium niobate glass-ceramics, J. Eur. Ceram. Soc. 43 (2023) 966–973.
[34] G.Q. He, Y.J. Liu, Y.H. He, Y. Wu, J. Liang, H.F. Zhou, Sintering behavior, phase composition, microstructure and dielectric properties of $SrSm_2O_4$ microwave ceramics, J. Alloys Compd. 924 (2022).
[35] C.Y. Tsao, W.H. Tuan, K.C. Feng, De-sintering of $Ba_5Nb_4O_{15}$ ceramic and its influence on microwave characteristics, J. Eur. Ceram. Soc. 37 (2017) 1517–1521.
[36] C.Z. Yin, K. Du, M. Zhang, C.C. Li, W. Lei, W.Z. Lu, Novel low-ε_r and lightweight $LiBO_2$ microwave dielectric ceramics with good chemical compatibility with silver, J. Eur. Ceram. Soc. 42 (2022) 4580–4586.
[37] W.J. Guo, Z.Y. Ma, Y.G. Chen, Y.T. Lu, Z.X. Yue, A case study of Al-doped $Ca_{0.6}Sm_{0.27}TiO_3$ ceramics, J. Eur. Ceram. Soc. 42 (2022) 4953–4961.
[38] R. Lowndes, M. Deluca, F. Azough, R. Freer, Probing structural changes in $Ca_{(1-x)}Nd_{2x/3}TiO_3$ ceramics by Raman spectroscopy, J. Appl. Phys. 113 (2013).
[39] H. Zheng, I.M. Reaney, R. Ubic, V.M. Ferreira, Raman spectroscopy of $CaTiO_3$-based perovskite solid solutions, J. Mater. 19 (2004) 488–495.
[40] J.C. Ma, Y. Xiong, X. Zhang, Z. Xiong, B. Tang, Studies of phase transitions, Raman spectra and microwave dielectric properties of perovskite-structured $(Na_{1-x}Li_x)_{0.5}Nd_{0.5}TiO_3$ ceramics, J. Mater. Sci. Mater. Electron. 34 (2023).
[41] Y.X. Hao, Y.P. Pu, J.B. Zhang, H.C. Xie, X. Lu, Q. Pan, L. Zhang, B. Wang, Ultra-high energy storage efficiency achieved through the construction of interlocking microstructure and excitation of depressor effects, Compos. B Eng. (2025) 290.
[42] N. Xu, Y.P. Pu, B. Wang, Enhanced mechanical and dielectric behavior of $BaTiO_3$/Cu composites, Ceram. Int. 38 (2012) 141–146.
[43] H. Hyuga, Y. Hayashi, T. Sekino, K. Niihara, Fabrication process and electrical properties of $BaTiO_3$/Ni nanocomposites, Nanostruct. Mater. 9 (1997) 547–550.
[44] S.M. Luo, Y.J. Zhang, Q. Wang, T. Que, Y. Lu, Y.T. Shan, H.Q. Zhou, Effects of $(Zn_{1/3}Nb_{2/3})^{4+}$ co-substitution on structure and microwave dielectric properties of $0.75CaTiO_3$–$0.25SmAlO_3$ ceramics, J. Mater. Sci. Mater. Electron. 34 (2023).
[45] Y.Y. Liu, M.S. Fu, H.J. Guo, X. Ma, L. Ni, Structure and microwave dielectric properties of 1:1 ordered $Nd[(Mg_{1-x}Zn_x)_{1/2}Ti_{1/2}]O_3$ complex perovskite ceramics, Ceram. Int. 48 (2022) 23044–23050.
[46] M.J. Xie, X. Li, Y.M. Lai, C. Qi, J. Yin, W.P. Gong, Y.X. Li, Q. Liu, C.S. Wu, Phase evolution and microware dielectric properties of high-entropy spinel-type $(Mg_{0.2}Co_{0.2}Ni_{0.2}Li_{0.4}Zn_{0.2})Al_2O_4$ ceramics, J. Eur. Ceram. Soc. 44 (2024) 284–292.
[47] M. Wei, M.F. Zhou, B. Liu, C.C. Hu, Y.H. Cheng, K.X. Song, Low permittivity MgF_2-LiF ceramics with ultra-low dielectric loss for ULTCC applications, J. Eur. Ceram. Soc. 44 (2024) 6495–6500.
[48] D.Q. Chen, X.W. Zhu, S.Y. Xiong, G.B. Zhu, L.J. Liu, J. Khaliq, C.C. Li, Tunable microwave dielectric properties in rare-earth niobates via a high-entropy configuration strategy to induce ferroelastic phase transition, ACS Appl. Mater. Interfaces 15 (2023) 52776–52787.
[49] A.J. Bosman, E.E. Havinga, Temperature dependence of dielectric constants of cubic ionic compounds, Phys. Rev. 129 (1963) 1593–1600.
[50] L. Shi, X.Y. Wang, R. Peng, Y.C. Lu, C. Liu, D.N. Zhang, H.W. Zhang, Bond characteristics and microwave dielectric ceramic of rare-earth tantalite $NdTaO_4$ ceramic, Ceram. Int. 48 (2022) 30101–30106.
[51] Z. Wang, J.T. Kang, Y. Xue, R.H. Ye, T. Zhao, The structural characteristics and microwave dielectric properties of $(Mg_{0.5}Ti_{0.5})^{3+}$ substituted $Sr_{0.6}Ca_{0.4}LaAlO_4$ ceramics, Ceram. Int. 50 (2024) 985–993.
[52] Y. Jiang, G.F. Wu, M.M. Mao, R. Muhammad, W.Q. Sheng, B. Liu, K.X. Song, Deeper insights into dodecahedron distortion and microwave dielectric properties of $Y_{3-x}R_xAl(_{Oct})_2Al(_{Tet})_{3-x}Si_xO_{12}$ (x = 0.1–0.5; R = Mg, Ca) garnet-type ceramics, Ceram. Int. 49 (2023) 23334–23339.
[53] J.T. Kang, Z. Wang, Y. Xue, R.H. Ye, T. Zhao, Z. Liu, Crystal structure, bond characteristics and enhanced microwave dielectric properties of $Sr_{0.6}Ca_{0.4}LaAl_{1-x}(Zn_{0.5}Ti_{0.5})_xO_4$ ceramics, Ceram. Int. 49 (2024) 23334–23339.
[54] H.C. Xiang, L. Yao, J.Q. Chen, A.H. Yang, H.T. Yang, L. Fang, Microwave dielectric high-entropy ceramic $Li(Gd_{0.2}Ho_{0.2}Er_{0.2}Yb_{0.2}Lu_{0.2})GeO_4$ with stable temperature coefficient for low-temperature cofired ceramic technologies, J. Mater. Sci. Technol. 93 (2021) 28–32.
[55] F.L. Lin, B. Liu, Q.W. Zhou, Y.H. Cheng, K.X. Song, Novel non-equimolar $SrLa(Al_{0.25}Zn_{0.125}Mg_{0.125}Ga_{0.25}Ti_{0.25})O_4$ high-entropy ceramics with excellent mechanical and microwave dielectric properties, J. Eur. Ceram. Soc. 43 (2023) 6909–6915.
[56] K. Liu, H.W. Zhang, C. Liu, J. Li, L. Shi, X.Y. Wang, D.N. Zhang, Crystal structure and microwave dielectric properties of $(Mg_{0.2}Ni_{0.2}Zn_{0.2}Co_{0.2}Mn_{0.2})_2SiO_4$ - a novel high-entropy ceramic, Ceram. Int. (2022) 48.
[57] S.S. Li, Y. Ren, G. Chen, M.C. Du, Y.H. Wang, L. He, L.M. Zhou, P. Ye, C.L. Fu, The effect of Ti/Ba ratio on the microstructures and microwave dielectric properties of $BaTi_4O_9$–$Ba_2Ti_9O_{20}$ composite ceramics, Ceram. Int. 50 (2024) 20080–20087.
[58] X. Meng, Y.B. Fan, A. Zhang, S.Q. Zheng, B.X. Ji, Q. Li, W.J. Wang, H.Q. Fan, Structure refinement, Raman vibration, impedance spectra and microwave dielectric properties of $MgZrNb_{2-x}(Ge_{1/2}W_{1/2})_xO_8$ ($0.02 \leq x \leq 0.08$) ceramics with the high quality factor, Ceram. Int. 50 (2024) 6395–6402.
[59] J. Bao, W.J. Guo, H.D. Kimura, Y.P. Zhang, J.L. Du, Y.Y. Zhou, Y. Ma, H.T. Wu, Z. X. Yue, Crystal structures, bond characteristics, and dielectric properties of novel middle-εr Ln_3NbO_7 (Ln=Nd, Sm) microwave dielectric ceramics with opposite temperature coefficients, Ceram. Int. 48 (2022) 36900–36907.
[60] L.T. Liu, L.G. Wang, J.L. Du, Z.B. Feng, H.T. Wu, X.Y. Zhang, P.J. Gong, Eu_3NbO_7: Novel middle-dielectric constant microwave dielectric ceramic with monoclinic structure, Ceram. Int. 47 (2021) 13221–13226.
[61] G.B. Zhu, F.R. Li, D.Q. Chen, X.W. Zhu, S.Y. Xiong, H.X. Xiao, L.J. Liu, C.C. Li, Effect of raw material pretreatment and ionic radius on the preparation and microwave dielectric properties of Re_2TiO_5 ceramics, Ceram. Int. 50 (2024) 19194–19201.
[62] X.W. Hu, J.W. Chen, J. Li, H.C. Xiang, Y. Tang, L. Fang, Contrasting microwave dielectric properties of zircon-structured $AEuV_2O_8$ (A = Bi, La) ceramics, J. Eur. Ceram. Soc. 42 (2022) 7461–7467.
[63] J.M. Chen, T.F. Hong, Y.L. Chai, Y.C. Lee, Influence of ZrO_2 doping on the microwave dielectric properties and microstructures of $Bi_2Mo_2O_9$ ceramics, Ceram. Int. 41 (2015) S576–S581.
[64] K.G. Wang, H.F. Zhou, X.W. Luan, S. Hu, X.J. Zhou, J.J. Deng, S.X. Li, Microwave dielectric properties of $LiSmTa_4O_{12}$ ceramics with A-site deficient perovskite structure, Mater. Lett. 274 (2020).
[65] J.Q. Chen, Y. Tang, J. Li, H.C. Xiang, C.C. Li, X.R. Xing, L. Fang, Structure and microwave dielectric properties of $Ba_3Nb_{4-4x}Ti_{4+5x}O_{21}$ ceramics with medium-high permittivity, J. Alloys Compd. 820 (2020).
[66] Q. Wan, Z.P. Li, H.F. Wang, G. Xiong, G. Wang, Crystal structure and microwave dielectric characteristics of novel $Ba(Eu_{1/5}Sm_{1/5}Nd_{1/5}Pr_{1/5}La_{1/5})_2Ti_4O_{12}$ high-entropy ceramic, Crystals (2024) 14.
[67] T.B. Xie, Z.P. Xiong, Z. Liu, G.Y. Deng, X.W. Cheng, Excellent combination of compressive strength and ductility of $(CoCrFeNi)_x(Co_{0.26}Cr_{0.07}Fe_{0.16}Ni_{0.31}Hf_{0.4})$ high-entropy alloys, Mater. Des. 202 (2021) 109569.